Twelfth Australasian Fluid Mechanics Conference
The University of Sydney, Australia 1995

THREE-DIMENSIONAL MODE DEVELOPMENT IN LOW REYNOLDS NUMBER FLOW OVER A CYLINDER

Mark C. Thompson, Kerry Hourigan and John Sheridan
Department of Mechanical Engineering
Monash University
Clayton, Victoria AUSTRALIA

ABSTRACT

In this paper results from numerical simulations for the transition to three-dimensional flow for a circular cylinder wake are compared with experimental visualisations and data. The simulations were performed with a spectral-element method. Both shedding frequency and base suctions are predicted to within experimental error in the two-dimensional shedding regimes. The initial instability wavelength (mode A) closely matches the measured wavelength from experiments as does the second instability (mode B) which occurs at slightly higher Reynolds numbers. There are indications that the interaction of these two modes may suppress the period-doubling found in previous simulations.

INTRODUCTION

Recently, there has been renewed interest in the classic problem of flow past a circular cylinder and, in particular, the development of the three-dimensional instability. Considerable progress has been made, experimentally analytically and numerically, in understanding the details of the transition process. This problem is important because it is perhaps the simplest generic bluff-body wake flow system and results are likely to be relevant to other more complex wake flow systems. There is also the prospect of improving our understanding of the route to turbulence for wakes.

Karniadakis and Triantafyllou (1992) were among the first to predict the three-dimensional wake structures computationally. These authors found the critical Reynolds number for 3D transition ($Re \approx 200$) consistent with the experimentally determined value ($Re \approx 180$) (given the blockage effect of the narrow domain). More importantly, they suggest that the route to turbulence is via the classical period-doubling route from chaos theory. Since then Noack and Eckelmann (1994) have used a global Galerkin method to model the three-dimensional transition. Using a Floquet analysis based on this method they find that the transition Reynolds number is approximately 170 with the most unstable mode possessing a wavelength of about 1.8 cylinder diameters (D). This is broadly in agreement with their experimental result of approximately $1.7D$. In contrast, the instability modes observed by Williamson (1988), and subsequently by Mansy, Yang and Williams (1994), and Norberg (1994), possessed a spanwise wavelength of the order of 3–4D at the onset of three-dimensionality (mode A) and reduced to about $1D$ for $Re > 250$ (mode B). A recent paper by Henderson and Barkley (1995) using a Floquet analysis based on two-dimensional spectral element simulations has predicted the initial instability wavelength (mode A) to be about $4D$ and the transition Reynolds number to be about $Re = 190$. Thompson, Hourigan and Sheridan (1994) have computed the two instability modes using a spectral/spectral element code and have found the spanwise wavelength of the structures to be in agreement with the experimental findings of Williamson (1988), and the Floquet analysis of Henderson and Barkley (1995). Recently, Zhang *et al.* (1995) (including Noack and Eckelmann) used a finite volume method to look at the initial stages of the transition to three-dimensionality. They also found results more in line with the experimental findings for the two shedding modes. In addition, they find that a three-dimensional mode with a wavelength of approximately $2D$ can be induced by perturbing the flow in a certain way.

It is the purpose of this paper to explore the agreement (or otherwise) between the computational modelling, the semi-analytical results and the experimental measurements.

METHOD

The spectral-element method was used for the spatial discretisation of the unsteady incompressible Navier-Stokes equations which govern the flow. This is a Galerkin finite-element method which uses high-order Lagrangian interpolants within each element. The node points correspond to the integration points for Gauss-Legendre-Lobatto quadrature. This leads to particular efficiencies, such as diagonal *mass* matrices and significantly reduced cost for the evaluation of the integrals resulting from the application of the weighted residual technique. (These features are common to spectral methods). Other numerical devices leading to computational efficiencies include *static condensation* which reduces the size of matrix subproblems resulting from the time discretisation.

The equations are discretised in time using a classical three-step splitting technique as described in Karnidakis *et al.* (1991). The substeps treat the convection, pressure and diffusion terms respectively. A higher-order boundary condition is used for the pressure substep which ensures overall second-order temporal accuracy. Details of the method can be found in Karniadakis *et al.* (1991), Karniadakis and Triantafyllou (1992) and Thompson *et al.* (1995), at this conference.

For the three-dimensional simulations, the spanwise direction is treated using the Galerkin Fourier method and hence periodic boundary conditions are imposed. This has implications for the wavelengths that can be represented; this point will be addressed later.

RESULTS

Figure 1 shows a close-up in the vicinity of the cylinder of a typical spectral-element mesh used for the simulations. For Reynolds numbers in the range 100–200 the outer boundary needs to be of the order of 10–15 cylinder diameters from the cylinder to predict the Strouhal-Reynolds number variation to within about 1%. Some care was exercised in placing and sizing the elements to give good resolution. Typically 8th to 12th order polynomial interpolants were used within the elements to resolve the velocity field.

Since the spectral-element method only enforces continuity in the function (velocity field) but not the derivatives at element boundaries, inadequate resolution is usually reflected in discontinuities in derivative quantities. Thus, a useful indication of adequate resolution is provided by examining the continuity of the vorticity field across element boundaries. This is likely to be a stronger test than, for example, examining the variation of Strouhal shedding frequency with polynomial interpolation order (as used by Karniadakis and Triantafyllou (1992)). The latter may only be a function of providing adequate resolution in a limited region (such as near the cylinder) while the former can provide a global accuracy indicator.

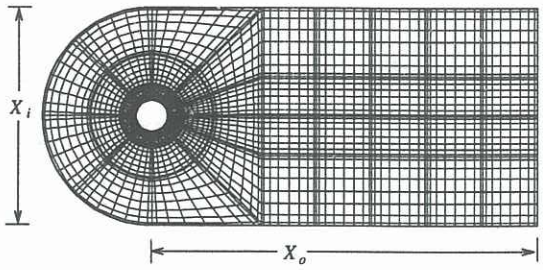

Figure 1: Two-dimensional spectral-element mesh in the neighbourhood of the cylinder. For this mesh eighth-order polynomial interpolating functions are used in each element in each direction.

Two-dimensional simulations reproduce the Strouhal-Reynolds number relationship and the variation of base suction with Reynolds number in the two-dimensional regime. The base suction variation is shown in Figure 2. The base suctions agree well with the experimental results in the two-dimensional shedding regime. After transition the three-dimensional simulations predict there is a drop in base suction in line with the experimental observations. Experimentally, the transition Reynolds number depends sensitively on end conditions so it is difficult to perform a quantitative comparison.

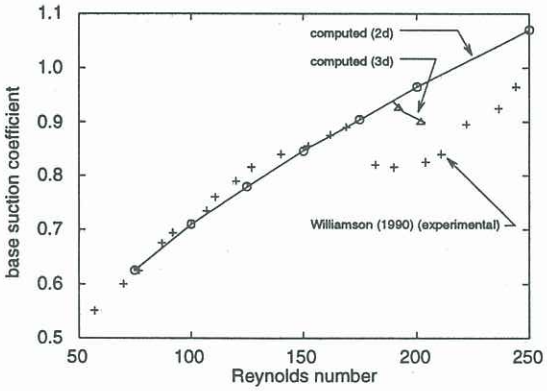

Figure 2: Variation of base suction with Reynolds number. The circles and solid line show the results from a two-dimensional simulation and the crosses are experimental results obtained by Williamson and Roshko (1990). The drop in the suction at $Re = 180$ is due to the onset of three-dimensional shedding.

As described previously, the experimental flow visualisations indicate that the development of the three-dimensionality involves at least two clearly defined stages. It is found that just after the onset of three-dimensional flow at a Reynolds number close to 200, streamwise vortex structures form which are periodic and have a spanwise wavelength of 3–4 cylinder diameters. This is called Mode A by Williamson

(1988) and has since been verified by others (Mansy, Yang and Williams, 1994, Norberg 1994). At a Reynolds number of order 250 a second mode, Mode B, begins to take over. This mode is less periodic (or more affected by small perturbations) and has a spanwise wavelength close to one cylinder diameter. The initial stage (mode A) may not even occur experimentally unless the aspect ratio of the cylinder is large or special end conditions are employed to reduce end effects. In both cases, the three-dimensionality manifests itself as streamwise vortex loops between the predominantly two dimensional spanwise vortex rollers which make up the vortex street.

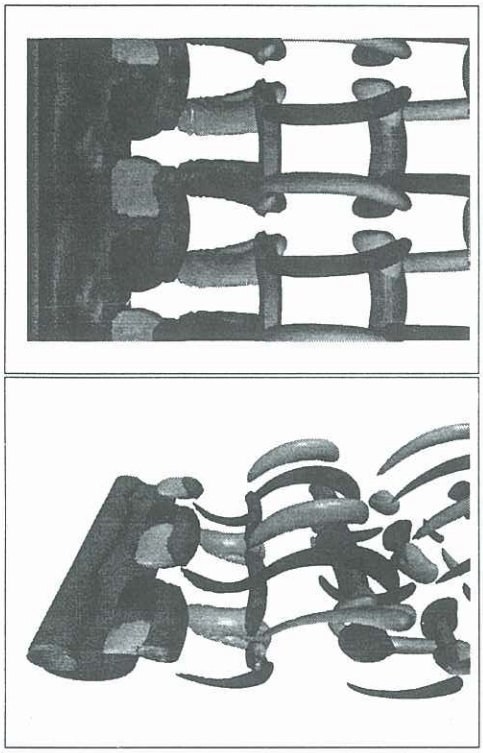

Figure 3: Top: Plan view of mode A three-dimensional flow at $Re = 210$. The vertically aligned (spanwise) structures are pressure isosurfaces highlighting the two-dimensional vortex street and the streamwise structures linking the spanwise vortices are isosurfaces of positive and negative streamwise vorticity. The spanwise wavelength of the streamwise structures is πD. Bottom: Perspective view showing the same strucures. Flow is from left to right.

Figure 3 is an isosurface plot showing pressure isosurfaces (-0.3 ρu_∞^2) indicating the placement of the two-dimensional spanwise vortex rollers, and isosurfaces of streamwise vorticity ($\pm$ 0.6 u_∞/D) which link the spanwise vortex structures. The Reynolds number is 210. This corresponds to the mode A shedding as defined by Williamson (1988). The flow is from left to right. The cylinder is obscured by the vortex sheet attached to it. The span shown is 2π diameters which corresponds to twice the computational span. The predominantly two-dimensional spanwise vortex rollers remain but are *connected* by streamwise vortex loops. These structures form in the region of high strain between the Strouhal vortices as they are forming. The Reynolds number in this case is just in excess of the transition Reynolds number and the shedding is periodic. (Simulations have been performed with increased span sizes to verify this result.) The simulations also produce Mode B for Reynolds numbers close to 250. This mode appears to be maintained for much higher Reynolds numbers and can be seen, for example, in the visualisations of Wu *et al.* (1994) at $Re = 1000$, and Wei and Smith (1986) at $Re = 4350$. The spanwise wavelength of the three-dimensional structures is almost constant for $Re < 1000$. For much larger Reynolds numbers the flow is more sensitive and turbulent in the near wake and the wavelength is more difficult to determine accurately.

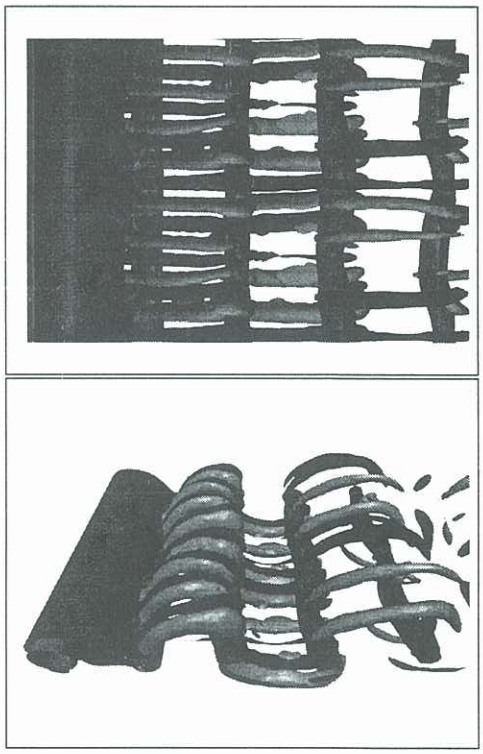

Figure 4: Same as for previous figure but for a Reynolds number of 250. The three-dimensional structures correspond to mode B shedding.

The recent Floquet analysis by Barkley and Henderson (1995) indicates that the development of Mode A is due to a natural instability of the two-dimensional Strouhal shedding at a Reynolds number of about 190 and the instability wavelength is close to $4D$. Both the present results, and the experimental results of several experimental groups (Williamson (1988), Mansy, Yang and Williams (1994), and Norberg (1994)) agree with the Floquet analysis. However, since there has been disagreement in the literature on the instability wavelength both numerically and experimentally, (Noack and Eckelmann (1994),

Noack, König and Eckelmann (1993)), this point was further addressed by performing numerically experiments to determine the growth rate of different wavelengths. From a perturbed two-dimensional solution, three-dimensional simulations were performed for different span sizes including only the lowest Fourier modes. The Reynolds number was 250. Figure 5 shows the results. The growth rate (α) is plotted against the wavelength of the Fourier mode. The wavelength is unstable only if the amplitude multiplier (α) is greater than unity. The figure shows the maximum growth rate occurs at about $3.4D$—consistent with the observed experimental value (3–$4D$) and in line with the Floquet analysis ($3.96D$). These calculations were done on a narrow domain $X_i = 7D$, so blockage may affect the result. An interesting point is that only modes with wavelengths in the range 2.7—$6D$ appear to be unstable. This would seem to indicate that the mode B instability will only occur after the mode A wavelength has been established. Of course, end-effects or very high perturbation levels may provide other paths for the development of the mode B structures.

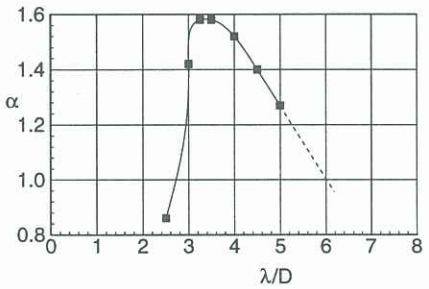

Figure 5: Amplitude multiplier (α) as a function of spanwise wavelength for the numerical stability analysis. The instability will grow for $\alpha > 1$. Simulations at lower wavelengths suggest that the multiplier is less than unity for $\alpha < 2.7D$. The Reynolds number is 250.

Another important issue is the nature of the transition to turbulence. Karniadakis and Triantafyllou (1992) used a spectral-element simulation to try to resolve the route to turbulence in wake flow systems. They found that the wake undergoes a series of period-doublings and speculated that wake turbulence is due to the classical period-doubling route to chaos. Recent experimental results have found some evidence to support their conjecture (Williams *et al.* 1995); however, their results (and conclusions) were influenced by using a span size that was too small to capture Mode A. With the inclusion of Mode A, it is not clear whether period-doubling occurs. Two simulations were performed with equivalent spatial resolution but with two different span sizes. The first used a span size of $\pi D/2$ as used by Karniadakis and Triantafyllou (1992) and Tomboulides *et al.* (1992). The Reynolds number was 250. Figure 6 shows a time trace of the streamwise velocity component at a point $1D$ downstream from the centre of the cylinder. Period-doubling can be seen clearly. The second simulation used a span size of πD. Here it is not clear whether period-doubling is still occurring. At this Reynolds number the flow does not settle down to a periodic flow and it would seem that the complex interaction occurring between mode A and mode B at least masks the period-doubling, if not suppressing it.

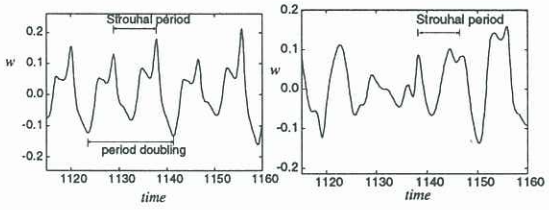

Figure 6: Spanwise velocity component as a function of time at a point in the wake approximately $1D$ downstream of the cylinder center. Left: Span size = $\pi D/2$. Period-doubling is clearly visible. Right: Span size = πD. Period-doubling suppressed or obscured. The Reynolds number is 250.

REFERENCES

BARKLEY, D. & HENDERSON, R.D., 1995, *J. Fluid Mech.*, submitted.

KARNIADAKIS, G. E. & TRIANTAFYLLOU, G. S., 1992, *J. Fluid Mech.* **238**, 1–30.

KARNIADAKIS, G.E., ISRAELI, M. & ORSZAG, S.A., 1991, *J. Comp. Phys.*, 97, 414–443.

MANSY, H., YANG, PAN-MEI, & WILLIAMS, D.R., 1994, *J. Fluid Mech.* **270**, 277-296.

NOACK, B. R. & ECKELMANN, H., 1994, *Phys. Fluids* **6**, 124–142.

NOACK, B.R., KÖNIG, M., & ECKELMANN, H., 1993, *Phys. Fluids*, A 5, 1279.

NORBERG, C., 1994, *J. Fluid Mech.* **258**, 287–316.

THOMPSON, M.C., HOURIGAN, K. & SHERIDAN, J., 1994, International Colloquium on Jets, Wakes and Shear Layers, DBCE, CSIRO, April 1994, Melbourne, Australia.

WILLIAMS, D.R., MANSY, H. & ABOUTEL-FOTOUH, A., 1995, PHYS. FLUIDS, submitted.

WILLIAMSON, C. H. K., 1988, *Phys. Fluids* **31**, 3165.

WILLIAMSON, C.H.K. & ROSHKO, A., 1990, *Z. Fluggwiss. Weltraumforsch*, 14, 38–46.

WEI, T. & SMITH, C.R., 1986, *J. Fluid Mech.*, 169, 513–533.

WU, J., SHERIDAN, J., SORIA, J. & WELSH, M.C., 1994, *J. Fluids and Struct.*, 8, 621–635.

ZHANG, H.Q., FEY, U., NOACK, B.R., KÖNIG, M. & ECKELMANN, H., 1995, On the transition of the Cylinder Wake, *Phys. Fluids.*